

Frequency and Temperature Dependent Dielectric Response of Fe₃O₄ Nano-crytallites

M. Z. Ansar^{1*}, S. Atiq², K. Alamgir¹, and S. Nadeem¹

¹National Institute of Vacuum Science and Technology, NCP Complex, Islamabad, Pakistan

²Center of Excellence in Solid State Physics, University of Punjab Lahore, Pakistan

Received 11 February 2014, accepted in revised form 5 August 2014

Abstract

Magnetite nanoparticles have been prepared by using sol-gel auto combustion technique. The samples are prepared by using different concentrations of fuel. Structural characterization has been done using X-Ray diffraction technique and it was observed that fuel concentration can affect the structural properties of Magnetite nanoparticles. The dielectric properties for all the samples such as dielectric constant (ϵ'), dielectric tangent loss ($\tan \delta$) and dielectric loss factor (ϵ'') have been studied as a function of frequency and temperature in the range 10 Hz–20 MHz and it was found that these nanoparticles can be used in microwave devices because of their good dielectric behavior.

Keywords: Magnetite nanoparticles; X-Ray diffraction; Impedance Analyzer; dielectric response; Sol-gel.

© 2014 JSR Publications. ISSN: 2070-0237 (Print); 2070-0245 (Online). All rights reserved.

doi: <http://dx.doi.org/10.3329/jsr.v6i3.17938>

J. Sci. Res. 6 (3), 399-406 (2014)

1. Introduction

Magnetite nanoparticles have been extensively studied due to their enormous applications in research and development such as; magnetic sensors [1], high density magnetic recording media [2], printing ink [3], ferrofluids [4], magnetic resonance imaging [5], catalysis [6] and especially in biological labeling, tracking, imaging, detection, and separations because of their bio-compatibility and chemical stability [7]. Various methods have been devised to synthesize Fe₃O₄ such as sol-gel auto combustion, co precipitation, sono-chemical approach, micro emulsions technique, hydrothermal synthesis and thermal decomposition [8, 12]. In the present study sol-gel auto combustion technique has been used to prepare the nanoparticles. It is a simple technique, a significant saving in time and energy consumption over the traditional methods besides this method offers improved structural characteristics and more homogeneity [13].

* Corresponding author: zakaphy@gmail.com

The dielectric properties of Magnetite nanoparticles depend upon several factors like synthesis technique, grain size, frequency and temperature. We are only interested in frequency and temperature dependent dielectric response of Fe_3O_4 nanoparticles in this paper because Ferrites are used in microwave devices because they are good dielectrics and we want to use iron oxide in microwave devices.

2. Experimental Method

Three samples of iron oxide magnetic nanoparticles were prepared by using a novel sol-gel auto-combustion technique. In this method, a fuel agent is used which plays a significant role in determining the crystal structure of the material. In the present study, citric acid has been used as a fuel and its contents have been varied to affect the pH of the solution, and the consequent effect on the structure has been studied. All the reagents used were of analytical grade purity. The stoichiometric amounts of ferric nitrate [$\text{Fe}(\text{NO}_3)_3 \cdot 9\text{H}_2\text{O}$, Panreac Quima SA] and citric acid [$\text{C}_6\text{H}_8\text{O}_7 \cdot \text{H}_2\text{O}$, Panreac Quima SA] were taken as the starting material. The metal nitrate (MN) to citric acid (CA) ratio used was 1:1, 1:2 and 1:3, to make three samples, named as S1, S2 and S3, respectively. The reagents were dissolved separately in 50 ml of de-ionized water and then mixed to make a total volume of 100 ml, in each case. The solution was placed on a hot plate at a temperature of 90°C and stirred continuously using a magnetic stirrer. The whole set up was placed in an ESCO fume hood.

After the continuous stirring of about 1 h, the solution was converted into a gel. At this point, the stirrer was taken out of the beaker and the temperature of the gel was increased to 250°C . In about 20 min, the gel was burnt in a self-propagating exothermic reaction. The final product was a loose and fluffy powder which was grinded using an Agate mortar and pestle to make the grain size uniform. The powder was sintered in an inert atmosphere for 10 h at 600°C in order to ensure complete combustion. All other samples were prepared following the same procedure.

Phase analysis and crystal structure was determined using X-ray diffraction (XRD). The dielectric properties, i.e. dielectric constant, tangent loss and dielectric loss factor were obtained using a Wayne Kerr Impedance analyzer.

3. Results and Discussion

3.1. XRD results

Fig. 1 shows the diffraction patterns of all the three samples obtained using XRD. Fig. 1(a) shows the diffraction pattern of the sample (S1), prepared using MN to CA ratio of 1:1. The peaks at $2\theta = 30.15^\circ, 35.43^\circ, 43.23^\circ, 57.06^\circ$ and 62.69° were matched with the ICSD ref. no. 01-072-2303, corresponding to the cubic structure of magnetite (Fe_3O_4), with space group $\text{Fd}\bar{3}\text{m}$ and lattice parameter, $a = 8.400 \text{ \AA}$. γ -phase of Fe_2O_3 known as Maghemite has lattice parameters and some other physical characteristics very close to

Magnetite. The peak at $2\theta = 31.85^\circ$ could be indexed as (221), related to $\gamma\text{-Fe}_2\text{O}_3$, according to the ICSD ref. no. 00-24-0081. The peak at $2\theta = 45.67^\circ$ could not be indexed. It might be due to an unknown phase of iron oxide as this material has quite a lot of phases with lattice parameters very close to each other. This peak and the peak indebted to maghemite, both decreased in intensity as the concentration of the fuel agent was increased in the sample, S2. In addition, the peaks corresponding to the magnetite phase were increased in intensity. Further increase in the peaks corresponding to the Fe_3O_4 and decrease in the peaks related to $\gamma\text{-Fe}_2\text{O}_3$ were observed when the fuel concentration was further increased, keeping MN to CA ratio of 1:3. The results are quite in agreement with some previous reports [14].

Therefore, it is inferred that the organic fuel contents play a vital role in the evolution of magnetite phase using sol-gel auto-ignition route. Nevertheless, the presence of some impurity peaks at still higher contents of fuel agent reveals that it is very difficult to produce pure Fe_3O_4 nanoparticles by auto-combustion mechanism because nanoparticles oxidize at the combustion temperature and pressure [15].

The crystallite size was evaluated using Scherrer's formula given as,

$$\text{Crystallite size} = 0.9 \lambda / B \cos \theta \quad (1)$$

where ' λ ' is the wavelength of the $\text{Cu } K_\alpha$ radiation used during X-ray diffraction, ' B ' is the full width at half maximum in radians and ' θ ' is the Bragg's diffraction angle in degrees. The crystallite size was decreased from 27.96 ± 0.05 to 21.72 ± 0.05 nm as the fuel concentration was increased in the series of samples, as shown in Fig. 2.

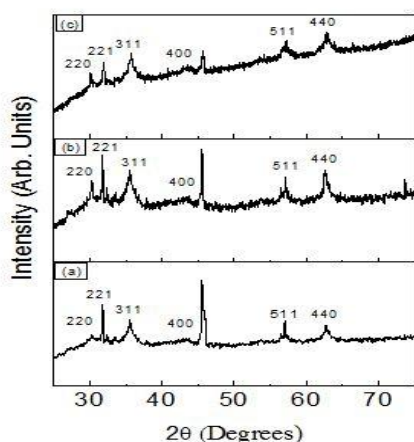


Fig. 1. XRD patterns of sample S1, S2 and S3.

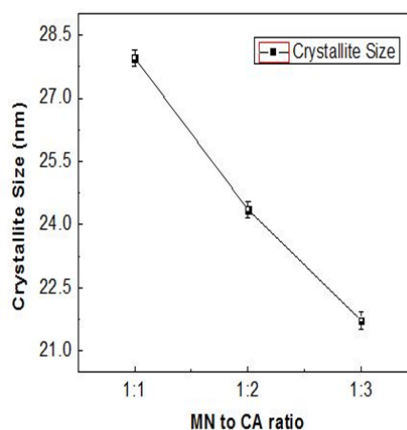


Fig. 2. Crystallite size as function of MN to CA ratio.

3.2. Frequency Dependent Dielectric Properties

10 mm in diameter pellets were used for the determination of dielectric properties of samples using an impedance analyzer. The corresponding thickness of the pellets was 0.90, 0.97 and 1.26 mm, respectively. The results of the dielectric constant, dielectric tangent loss and the dielectric loss factor as a function of frequency have been plotted in Figs. 3-5, respectively.

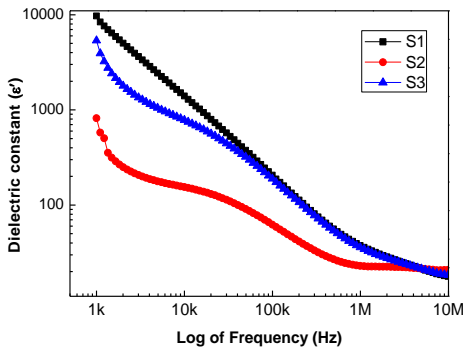


Fig. 3. Dielectric constant as a function of log frequency.

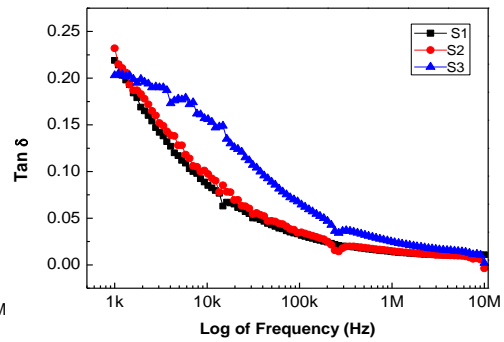


Fig. 4. Dielectric constant as a function of log frequency.

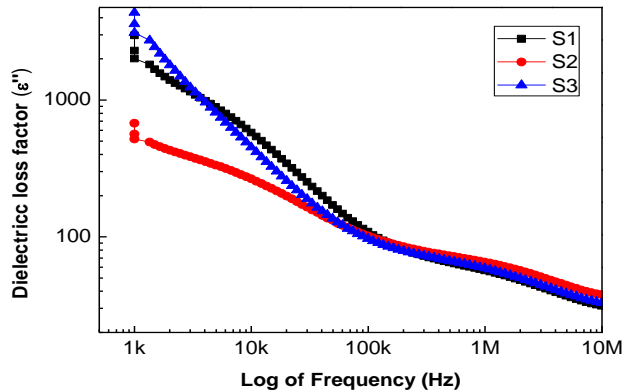


Fig. 5. Dielectric loss factor of samples S1, S2, S3 as function of log of frequency.

It can be easily interpreted from the plots that like other ferrites the Fe_3O_4 nanoparticles exhibit same trend, as having high values of dielectric constant, tangent loss and dielectric loss factor at low frequencies and decrease with the increase in frequency while reaching to a constant saturated value at high frequencies, depicting a frequency

independent behavior. This phenomenon can be explained on the basis of Koop's theory [16]. According to this theory, the dielectric structure was said to be composed of grains and grain boundaries in which grains were conductor while grain boundaries were non-conductive. This was also suggested by Maxwell and Wagner [17, 18]. The theory states that when the electric field is applied on a dielectric material, its atoms need a finite time to align themselves in the direction of field. This time is known as relaxation time and its precise value is 10^{-9} sec. As the frequency of electric field increases, a point is reached when charge carriers of dielectric do not align themselves in accordance with the field and so polarization cannot achieve its saturation value. The value of dielectric constant decreases and when we further increase the frequency, the dielectric constant becomes independent of frequency. To explain these trends, the effect of defects and dislocations in the samples might also be taken into account. These defects activate interfacial polarizations at low frequencies. Due to this polarization, the dielectric constant is higher at low frequencies. The same behavior has also been reported in literature [19, 21].

In addition, it has intensively been investigated that the dielectric properties of ferrites are dependent upon several other factors, including the method of preparation, chemical composition, grain structure and grain size of the ferrite nanoparticles [13]. This may be explained qualitatively by the fact that electronic exchange between ferrous and ferric ions in ferrites cannot follow the frequency of externally applied alternating field beyond a critical frequency value [22].

3.3. Temperature Dependent Dielectric Properties

The temperature dependent dielectric properties are calculated by precision impedance analyzer which is attached with a heater. The samples are placed in the heater and their response is taken at different temperatures. Temperature dependent dielectric constant, dielectric tangent loss and dielectric loss factor have been plotted in Figs. 6, 7 and 8. In these plots the frequency was treated as constant i.e. 10 kHz.

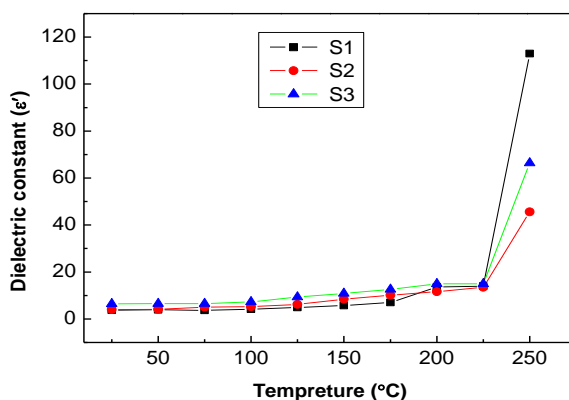


Fig. 6. Temperature dependent dielectric constant of samples S1, S2 and S3.

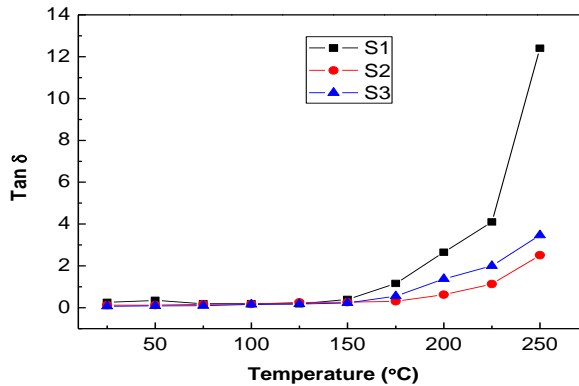


Fig. 7. Temperature dependent dielectric tangent loss of S1, S2 and S3.

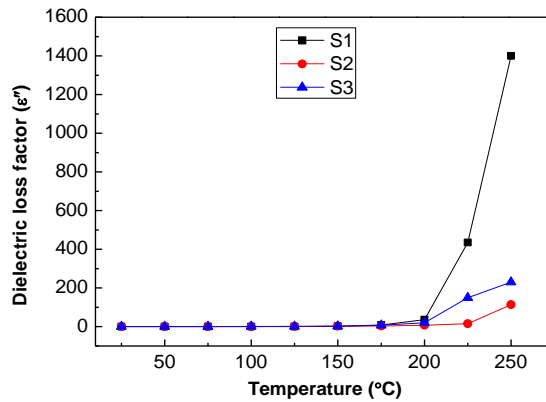


Fig. 8. Temperature dependent dielectric loss factor of S1, S2 and S3.

The behavior of dielectric properties with temperature is different over different temperature ranges i.e. at low and high temperature. It is evident from the graphs that the dielectric constant, dielectric tangent loss and dielectric loss factor are low at low and room temperature range and remain independent of temperature. In high temperature range the dielectric properties rise suddenly and reach a maximum value. This kind of behavior is in agreement with well-known ferrites. The same trends have also been reported in literature for other well-known ferrites [23, 25].

The basic reason of the independency of dielectric constant in low temperature range is that impurities remain localized in this range and so conduction is not easy while at high temperature impurities are no more localized and hence conductivity of the material is increased. In case of ionic solids, electrons of the material also become free and contribute to conduction. This results in high polarization of the material; hence value of dielectric constant is increased with increase in temperature [23].

This fact can also be explained on the basis of Koop's model postulates that crystalline solids are made up of grains and grain boundaries, such that grains have low resistivity and grain boundaries have high resistivity. At low and room temperature range, the effect of grain boundaries is dominant and that is why the dielectric properties have small magnitudes and are constant. As the temperature is increased, the role of grains becomes more and more effective and we see a sharp increase in the dielectric properties.

4. Conclusion

Fe₃O₄ nanoparticles were successfully synthesized by sol-gel auto-combustion route method. XRD results indicate that the Magnetite nanoparticles have face-centered cubic structure and their size and purity varies with the concentration of fuel used and as the concentration of fuel was increased the nanoparticles become purer and the crystallite size was also decreased. Frequency and temperature dependent dielectric response has been recorded by Precision Impedance Analyzer and it was found that the dielectric properties of iron oxide were decreased suddenly when frequency was increased keeping the temperature constant and when temperature was increased by keeping frequency constant the behavior of Magnetite nanoparticles resembles with well-known ferrites. So, by going through all these results iron oxide nanoparticles can also be used in microwave devices just like other ferrites.

References

1. H. Zeng, J. Li, J. P. Liu, Z. L. Wang, and S. Sun, *Nature* **420**, 395 (2002).
<http://dx.doi.org/10.1038/nature01208>
2. C. T. Black, C. B. Murray, R. L. Sandstrom, and S. Sun, *Science* **290**, 1131 (2000).
<http://dx.doi.org/10.1126/science.290.5494.1131>
3. T. Atarashi, T. Imai, and J. Shimoizaka, *J. Magn. Magn. Mater.* **85**, 3 (1990).
[http://dx.doi.org/10.1016/0304-8853\(90\)90004-A](http://dx.doi.org/10.1016/0304-8853(90)90004-A)
4. K. Raj, B. Moskowitz, and R. Casciari, *J. Magn. Magn. Mater.* **149**, 174 (1995).
[http://dx.doi.org/10.1016/0304-8853\(95\)00365-7](http://dx.doi.org/10.1016/0304-8853(95)00365-7)
5. L. X. Tiefenauer, A. Tschirky, G. Kühne, and R. Y. Andres, *Magn. Reson. Imaging* **14**, 391 (1996). [http://dx.doi.org/10.1016/0730-725X\(95\)02106-4](http://dx.doi.org/10.1016/0730-725X(95)02106-4)
6. D. M. Huang, D. B. Cao, Y. W. Li, and H. J. Jiao, *J. Phys. Chem. B* **110**, 13920 (2006).
<http://dx.doi.org/10.1021/jp0568273>
7. J. M. Nam, C. S. Thaxton, and C. A. Mirkin, *Science* **301**, 1884 (2003).
<http://dx.doi.org/10.1126/science.1088755>
8. Z. Hua, Y. Deng, K. Li, and S. Yang, *Nanoscale Res. Lett.* **7**, 129 (2012).
<http://dx.doi.org/10.1186/1556-276X-7-129>
9. Y. Wei, B. Han, X. Hu, Y. Lin, X. Wang, and X. Deng, *Procedia Eng.* **27**, 632 (2012).
<http://dx.doi.org/10.1016/j.proeng.2011.12.498>
10. R. Vijayakumar, Y. Kolytipin, I. Felner, and A. Gedanken, *Mater. Sci. Eng. A* **286**, 101 (2000).
[http://dx.doi.org/10.1016/S0921-5093\(00\)00647-X](http://dx.doi.org/10.1016/S0921-5093(00)00647-X)
11. D. E. Zhang, Z. W. Tong, S. Z. Li, X. B. Zhang, and A. Ying, *Mater. Lett.* **62**, 4053 (2008).
<http://dx.doi.org/10.1016/j.matlet.2008.05.023>
12. C. Y. Haw, F. Mohamed, C. H. Chia, S. Radiman, S. Zakaria, N. M. Huang, and H. N. Lim, *Ceram. Int.* **36**, 1417 (2012).

13. Z. Ullah, S. Atiq, and S. Naseem, *J. Sci. Res.* **5** (2), 235 (2013).
<http://dx.doi.org/10.3329/jsr.v5i2.11578>
14. K. Deshpande, A. Mukasyan, and A. Varma, *Chem. Mater.* **16**, 4896 (2004).
<http://dx.doi.org/10.1021/cm040061m>
15. J. Toniolo, A. S. Takimi, M. J. Andrade, R. Bonadiman, and C. P. Bergmann, *J. Mater. Sci.* **42**, 4785 (2007). <http://dx.doi.org/10.1007/s10853-006-0763-7>
16. B. D. Cullity, 'Introduction to Magnetic Materials' (Wesley Reading, New York, 1972) p. 355.
17. J. C. Maxwell, 'A Treatise on Electricity and Magnetism' (Clarendon Press, Oxford, 1982).
18. K. W. Wagner, *Ann. Phys.* **40**, 817(1913). <http://dx.doi.org/10.1002/andp.19133450502>
19. M. M. Rahman, P. K. Halder, F. Ahmed, T. Hossain, and M. Rahaman, *J. Sci. Res.* **4** (2), 297 (2012). <http://dx.doi.org/10.3329/jsr.v4i2.9752>
20. B. K. Kuanr and G. P. Srivastava, *J. Appl. Phys.* **75**, 6115 (1994).
<http://dx.doi.org/10.1063/1.355478>
21. G. Mu, N. Chen, X. Pan, H. Shen, and X. Gu., *Mater. Lett.* **62**, 840 (2008).
<http://dx.doi.org/10.1016/j.matlet.2007.06.074>
22. K. Iwauchi, *Jpn. J. Appl. Phys.* **10**, 1520 (1971). <http://dx.doi.org/10.1143/JJAP.10.1520>
23. A. S. Rahman, *Egypt. J. Solids* **29**, 131 (2006).
24. S. S. Shinde, and K. M. Jadhav, *Mater. Lett.* **37**, 63 (1998).
[http://dx.doi.org/10.1016/S0167-577X\(98\)00068-8](http://dx.doi.org/10.1016/S0167-577X(98)00068-8)
25. E. Ateia, *Egypt. J. Solids* **29**, 317 (2006).